
Dropout Strikes Back: Improved Uncertainty Estimation via Diversity Sampled Implicit Ensembles

Evgenii Tsymbalov*, Kirill Fedyanin* and Maxim Panov
 Skolkovo Institute of Science and Technology (Skoltech)
 Moscow, Russia

Abstract

Modern machine learning models usually do not extrapolate well, i.e., they often have high prediction errors in the regions of sample space lying far from the training data. In high dimensional spaces detecting out-of-distribution points becomes a non-trivial problem. Thus, uncertainty estimation for model predictions becomes crucial for the successful application of machine learning models in many applications. In this work, we show that increasing the diversity of realizations sampled from a neural network with dropout helps to improve the quality of uncertainty estimation. In a series of experiments on simulated and real-world data, we demonstrate that diversification via *determinantal point processes*-based sampling allows achieving state-of-the-art results in uncertainty estimation for regression and classification tasks. Importantly, our approach does not require any modification to the models or training procedures, allowing for straightforward application to any deep learning model with dropout layers.

errors can be mitigated with other models or techniques like human-in-the-loop.

Another important application for uncertainty estimation is active learning [Settles, 2012]. In active learning, we have a relatively small training set and a large unlabeled pool set. Labeling samples from the pool is supposed to be expensive, for example, manual labeling of images or accurate calculation of molecular energies with quantum mechanical models. Thus, it becomes critical to sample points in a way to obtain the most substantial improvement in model quality. The majority of sampling criteria in active learning are based on estimates of uncertainty, which makes it important to obtain high-quality uncertainty estimates.

There are several main approaches for uncertainty estimation for deep neural networks. Bayesian neural networks (BNN) and variational inference in particular represent a natural way for uncertainty estimation due to availability of well-defined posteriors, but they can be prohibitively slow for large-scale applications. The usage of dropout at the inference stage was shown to be good and efficient approximation to BNNs [Gal and Ghahramani, 2016, Gal, 2016]. The ensembles of independently trained models [Lakshminarayanan et al., 2017] were shown to have state-of-the-art performance in many tasks requiring uncertainty estimation [Snoek et al., 2019]. Recently, forcing models in ensembles to be more diverse was shown to improve results even further [Jain et al., 2019]. The drawback of ensembles is that we need to train and use multiple models that require additional resources, i.e. more memory to store models and more computing power for training.

In this work, we aim to develop a new approach for dropout-based uncertainty estimation. We treat a neural network with dropout as an implicit ensemble of models and propose to sample the most diverse models from it to improve the uncertainty estimation. As a particular realization of the general idea, we suggest sampling

1 Introduction

Uncertainty estimation (UE) recently become a very active area of research in deep learning. Neural networks usually are treated as black boxes, and in general, they are prone to overconfidence [Guo et al., 2017, Gal, 2016]. Uncertainty estimation methods aim to help overcome this drawback by identifying potentially erroneous predictions. This can be especially important for error-critical applications like medical diagnostics [Begoli et al., 2019] or autonomous car driving [Feng et al., 2018]. Detected

Equal contribution.

mask using the machinery of determinantal point processes (DPP) [Macchi, 1975, Kulesza et al., 2012] which are known to give diverse samples.

We summarize the main contributions of the paper as follows:

- We propose two DPP-based sampling methods for neural networks with dropout. Our approach requires to train only a single model and adds only small overhead on the inference stage compared to plain MC dropout.
- We compare different dropout-based approaches for uncertainty estimation with the ones based on ensembles in an extensive series of experiments for artificial and real-world regression and classification datasets, including applications of obtained uncertainty estimates to active learning. The results show state-of-the-art performance of proposed DPP-based approaches.
- We additionally show that inference with dropout for single models can be combined with ensembles to increase the quality of uncertainty estimation even further.

The rest of the paper is organized as follows. Section 2 introduces the proposed method for DPP-based sampling from neural networks with dropout. In Section 3, we show the efficiency of the proposed approach in the problem of uncertainty estimation. Section 4 gives an overview of the related work on uncertainty estimation for neural networks. Section 5 concludes the study and highlights some directions for future work.

2 Methods

2.1 Neural Networks with Dropout as Implicit Ensembles

We start by considering a standard fully connected layer in a neural network

$$S_i^h = \sum_{j=1}^{N_{h-1}} w_{ij}^h m_j^h O_j^{h-1}, \quad i = 1, \dots, N_h,$$

where O_i^h is an output of the h -th layer of the neural network given by a non-linear transformation $\sigma(\cdot)$ of the corresponding pre-activation S_i^h :

$$O_i^h = \sigma(S_i^h), \quad i = 1, \dots, N_h.$$

An application of dropout to neurons results in the following formula for the output:

$$O_i^h = \sigma\left(\sum_{j=1}^{N_{h-1}} w_{ij}^h m_j^h O_j^{h-1}\right), \quad i = 1, \dots, N_h,$$

where m_j^h are Bernoulli random variables with probability of 0 equal to p . Note that if an input variable of neural network is denote by \mathbf{x} , then output of every layer is a function of \mathbf{x} , i.e. $O_i^h = O_i^h(\mathbf{x})$.

Let us denote the vector of dropout weights m_j^h for the h -th layer by $\mathbf{m}_h = (m_1^h, \dots, m_{N_h}^h)^T$ and the full set of dropout weights by $\mathbf{M} = (\mathbf{m}_1, \dots, \mathbf{m}_K)$.

Thus, any neural network $\hat{f}(\mathbf{x})$ with dropout layers essentially has 2 sets of parameters: the full set of learnable weights \mathbf{W} and the set of dropout weights \mathbf{M} :

$$\hat{f}(\mathbf{x}) = \hat{f}(\mathbf{x} | \mathbf{W}, \mathbf{M}).$$

Let us have a neural network with dropout which was trained on some dataset giving weight estimates $\hat{\mathbf{W}}$. Then the dropout weights \mathbf{M} remain the free parameters and require selection at the time of inference:

$$\hat{f}(\mathbf{x} | \mathbf{M}) = \hat{f}(\mathbf{x} | \hat{\mathbf{W}}, \mathbf{M}).$$

The originally proposed [Hinton et al., 2012] and currently the standard choice is to take $\hat{\mathbf{M}} = \frac{1}{1-p} \mathbf{E}$, where p is the dropout rate used during training and \mathbf{E} is the matrix of all ones of the corresponding shape. Such an approach gives the fixed function $\hat{f}(\mathbf{x} | \hat{\mathbf{M}})$ which is known to give reasonably good performance despite being heuristic choice.

Recently, it was proposed to consider Bernoulli distribution as a prior over elements of a matrix \mathbf{M} [Gal and Ghahramani, 2016, Nalisnick et al., 2019], which results in a Bayesian model:

$$\hat{f}(\mathbf{x}) = \hat{f}(\mathbf{x} | \mathbf{M}), \quad \mathbf{M} \sim \text{Bernoulli}(1-p).$$

Within this approach one can sample some number T of i.i.d. realizations $\mathbf{M}_1, \dots, \mathbf{M}_T$ from the prior distribution and compute approximate posterior mean

$$\bar{f}_T(\mathbf{x}) = \frac{1}{T} \sum_{i=1}^T \hat{f}(\mathbf{x} | \mathbf{M}_i)$$

and variance

$$\bar{\sigma}_T^2(\mathbf{x}) = \frac{1}{T} \sum_{i=1}^T (\hat{f}(\mathbf{x} | \mathbf{M}_i) - \bar{f}_T(\mathbf{x}))^2.$$

Importantly, the approximate posterior variance $\bar{\sigma}_T^2(\mathbf{x})$ is a natural choice for the uncertainty estimate and was successfully used in the variety of applications such as out-of-distribution detection [Vyas et al., 2018] and active learning [Smith et al., 2018].

In this paper, we suggest a different approach, namely we treat $\hat{f}(\mathbf{x} | \mathbf{M})$ as an ensemble of models indexed by dropout masks \mathbf{M} . Such a view allows us to decouple inference from training and pose an intuitive question: what set of masks $\mathbf{M}_1, \dots, \mathbf{M}_T$ should one choose in order to obtain the best uncertainty estimate $\bar{\sigma}_T^2(\mathbf{x})$?

Importantly, here we do not limit the selection of masks to be samples from standard dropout distribution which in principle should allow to obtain better estimates. However, the design of mask selection procedure is a non-trivial problem, which we discuss below in detail.

Remark 1. *The standard approach in the literature is to consider an ensemble of models trained on different subsets of the data set or just from different random initializations giving the set of parameter estimates $\hat{\mathbf{W}}_1, \dots, \hat{\mathbf{W}}_T$ and corresponding approximations $\hat{f}(\mathbf{x} | \hat{\mathbf{W}}_i, \mathbf{M})$, $i = 1, \dots, T$. Similarly, one can compute the variance $\bar{\sigma}_T^2(\mathbf{x})$ which was shown to be a reasonable uncertainty estimate in practice [Smith et al., 2018]. The main drawback of this approach is the need to train and store T different models which might be very costly both in terms of computation and storage needed.*

2.2 Importance of Data-driven Mask Selection

In practice, many neurons in the network are highly correlated. For example, consider a correlation matrix of neurons in linear layer of a convolutional neural network, trained on CIFAR-10 (see Figure 1). The correlation was computed on 10^4 samples and clearly shows groups of highly correlated neurons. It suggests that sampling masks for such a layer completely at random might lead to many highly correlated neurons in the sample. This property is non-desirable as it leads to more correlated models in the ensemble. However, one may expect that the knowledge about the correlations between neurons can help to sample maximally diverse ensemble members.

2.3 Decorrelation Approaches

Let us consider a certain layer h of the network with dropout. Assume that we have access to the correlations $C_{ij}^{(h)} = \text{corr}_{\mathbf{x}}\{O_i^h(\mathbf{x}), O_j^h(\mathbf{x})\}$, $i, j = 1, \dots, N_h$. In practice we compute an empirical correlation based on some set of points which represents the data distribution well enough.

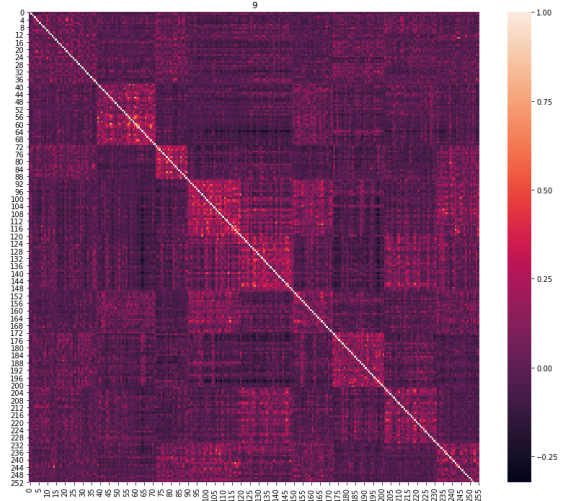


Figure 1: Correlation matrix C between the outputs of the neurons in a linear layer of the convolutional NN, trained on the CIFAR-10 dataset. Correlations are computed based on a set of 10^4 samples.

Finally, we obtain the correlation matrix:

$$C^{(h)} \in \mathbb{R}^{N_h \times N_h}$$

between the neurons of the h -th hidden layer. Below we discuss several approaches to sampling neurons in a way that the correlation between sampled neurons is as small as possible.

2.3.1 Naive Decorrelation

Since we want for the correlated neurons to be rarely sampled together, we suggest as a naive baseline to adjust the probability of sampling a given neuron based on the sum of absolute correlation values. Hence the probability $p_j^{(h)}$ of sampling the j -th neuron in a mask is

$$p_j^{(h)} \sim \text{softmax}\left(\left(\sum_{i=1}^{N_h} |C_{ij}^{(h)}|\right)^{-1}\right).$$

This approach makes neurons from large and highly correlated clusters to be sampled rarer. In Section 3, we show that such an approach indeed allows obtaining more accurate uncertainties compared to MC dropout. However, we propose a more principled approach, which allows for further improvement.

2.3.2 Sampling with Determinantal Point Processes

Determinantal Point Processes (DPPs) [Kulesza et al., 2012] are specific probability distributions over configurations of points that

encode diversity through a kernel function. They were introduced in [Macchi, 1975] for the needs of statistical physics and were used for a number of ML applications, see [Kulesza et al., 2012] for an overview. DPP can be seen as a probabilistic MaxVol algorithm [Goreinov et al., 2010, Çivril and Magdon-Ismail, 2009] of finding a maximal-volume submatrix.

We use correlation matrix $C^{(h)}$ as the likelihood kernel for DPP. Then, given a set S of selected points for a mask distribution $\mathbf{m}_h \sim DPP(C^{(h)})$, we obtain

$$\mathbb{P}[\mathbf{m}_h = S] = \frac{\det C_S^{(h)}}{\det[C^{(h)} + I]}, \quad h = 1, \dots, K,$$

where $C_S^{(h)} = [C_{ij}^{(h)}]_{i,j \in S}$, i.e., a square submatrix of $C^{(h)}$ obtained by keeping only rows and columns indexed by S . Finally, we sample T masks for each layer based on corresponding correlation matrices.

To better understand the DPP, let us come back to correlation matrix depicted in Figure 1. The probability for DPP to take highly correlated neurons into the sample S is low as in such case the corresponding determinant $\det C_S^{(h)}$ will have a small value. Thus, DPP tends to sample neurons from different clusters increasing the diversity of the ensemble.

2.3.3 k-DPP

The k-DPP is a variation of the DPP, conditioned to produce samples of fixed size $|S| = k$. With the cost of introducing an additional parameter it allows to tune the sampling procedure as the choice of k apparently has significant influence on the result. Motivated by clustered behaviour observed in real-world correlation matrices (see again Figure 1), we suggest taking k dependent on the rank of matrix $C^{(h)}$ and set

$$k = \pi \cdot \text{rank}(C^{(h)})$$

for some value $0 < \pi \leq 1$. In practice, matrix $C^{(h)}$ is never exactly low-rank and some notion of efficient rank should be used, see the details in Section 3.

Remark 2. *Importantly, if $\pi = 1$ and matrix $C^{(h)}$ is indeed block-structured and thus low-rank, the resulting sampling procedure for k-DPP will always give one neuron sampled from every block giving the same resulting approximation for all the samples. This behaviour contradicts our initial goals of diversifying samples; therefore, we took $\pi = 0.5$ in all our experiments.*

Remark 3. *We also note that DPP-based sampling may be considered from a fully Bayesian perspective, with*

DPP being a special prior on masks promoting diversity. We leave the study of this approach for future work.

2.4 Diversification for Uncertainty Estimation in Classification

Uncertainty estimation for classification is in some sense more challenging than for regression as there is no obvious candidate for uncertainty measure as variance of prediction. Some popular and efficient uncertainty estimates for classification are entropy of class probabilities [Shannon, 1948] which can be computed for a single model, and BALD [Houlsby et al., 2011] which is based on mutual information and requires an ensemble of models or a Bayesian model for computation.

In this work, we consider the *variation ratio* [Freeman, 1965] which was shown to be a useful uncertainty estimate in [Beluch et al., 2018]. If $f_m(\mathbf{x})$ is the number of ensemble models that predict the modal class category for an object \mathbf{x} , then a variation ratio is defined as

$$v(\mathbf{x}) = 1 - \frac{f_m(\mathbf{x})}{T}.$$

Importantly, the idea of this metric correlates well with our approach and we might expect an improvement from diversification.

3 Experiments

3.1 Models and Metrics

For the experiments, we consider all the UE methods discussed in the previous section: MC dropout baseline, decorrelation (see Section 2.3.1), DPP (Section 2.3.2) and k-DPP (Section 2.3.3). All the regression models were trained with RMSE as a loss function. See the details on model architectures and training procedures in Supplementary Material. For DPP-based methods, we use the DPPy implementation provided in [Gautier et al., 2019].

We should note that we do not compare with fully Bayesian approaches as we are focusing on the solutions which are applicable to the standard dropout-based models without changing model architecture and training procedure. On top of single models, we also consider a straightforward ensemble approach with NNs trained exactly the same way as single models from different initializations.

Also, for reference, we consider *oracle errors* which are simply the actual model errors at test points. Of course, the real errors are not available in practice; however it is natural to assume that good uncertainty estimates should

correlate with model’s errors. Thus, oracle errors can be used in experiments to compare the performance with considered approaches.

3.1.1 Metrics

We introduce the following metrics to assess the quality of the uncertainty estimation:

- **Log-likelihood (LL).** Following [Hernández-Lobato and Adams, 2015, Jain et al., 2019], we compute log-likelihood of Gaussian distribution with uncertainty estimates plugged in place of standard deviation.
- **Accuracy@K%.** Since one of the main applications of uncertainty estimation is active learning, we measure how many test samples out of K% having the largest estimated uncertainties are actually in the top K% of samples having the largest actual error.
- **Normalized Absolute Error@K% picked (NAE@K%).** The performance is measured by the mean error of the model computed for the samples having top K% uncertainty estimates. This value is then normalized by the mean of top K% oracle errors.

The performance measures used for assessing quality of uncertainty estimation in classification are discussed in Section 3.4.

3.2 2D Rings Toy Problem

In order to explore the performance of the considered uncertainty estimation approaches, we start with a relatively simple 2D function:

$$f(x, y) = \cos(\sin(xy) + \sin(x + y) + x - y + |x \cos y| \exp(\operatorname{sgn}(y)|y|^{0.5})).$$

We define four ring regions of interest which are shown in Figure 2:

- a sector containing all the training points (shown in purple);
- three out-of-distribution regions where we put test points: the blue sector region which complements the training sector, the red inner ring, and the green outer ring.

A NN with [128-128-256] architecture was trained on 1200 points in the training set, and the performance on

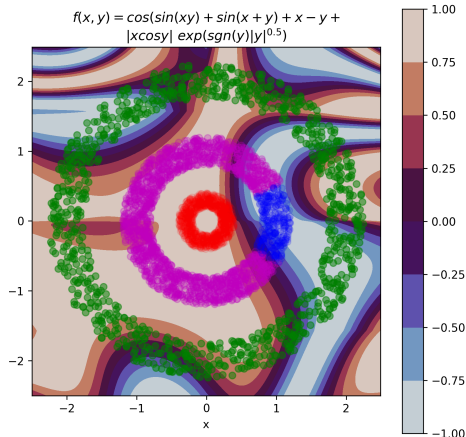


Figure 2: A 2D rings toy problem for UE testing. Purple points represent the training data, and red, blue, and green points represent different kinds of OOD data.

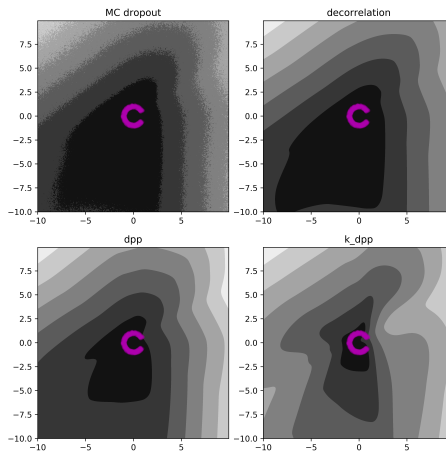


Figure 3: 2D Rings Toy Problem. Filled contour lines for the normalized UE as a function of input data. Purple region indicates the training data. Lighter regions indicate larger UE. k-DPP is more sensitive to the OOD data compared to other approaches.

the test regions was estimated using 300+ points in each as well.

We start the analysis by demonstrating how different UE approaches work with an extreme OOD data lying far from the training points. We show the isolines of the normalized UE metric for different approaches in Figure 3. We observe that DPP-based approaches are more sensitive to the OOD data compared to other approaches with k-DPP clearly showing the best result.

The more quantitative results are shown in Figure 4, where different approaches are compared using the NAE@10% metric. Note that the behaviour of the different uncer-

Table 1: Summary of the datasets used in UCI experiments section, see [Dua and Taniskidou, 2017].

Dataset name	Samples	Columns
boston	506	13
concrete	1030	8
energy	768	8
kin8nm ¹	8192	8
naval	11934	16
ccpp	9568	4
red wine	1599	11
yacht	308	6

tainty estimators varies, but k-DPP shows the results better corresponding to the actual (oracle) errors of the neural network in terms of the relative ordering of UEs for different regions of the design space.

3.3 Uncertainty Estimation for Real-World Regression Datasets

Similarly to [Jain et al., 2019], we run a series of experiments on various real-world regression datasets, see Table 1 for the list of datasets used. For this experiment, we used feed-forward NNs with leaky ReLU activation function [Maas et al., 2013] and 128-128-64 architecture. For each dataset, 50% was used for the training and 50% for testing. Multiple experiments are done via 2-fold cross-validation, and multiple runs / UE runs.

The quality of the UE procedures was assessed using the performance profile curves [Dolan and Moré, 2002]. Let q_a^p be an error measure of the a -th algorithm on the p -th problem. Then, denoting the performance ratio by $r_a^p = \frac{q_a^p}{\min_x(q_x^p)}$, we can define the Dolan-More curve as a function of the performance ratio factor $\tau \geq 1$:

$$\rho_a(\tau) = \frac{\#\{p: r_a^p \leq \tau\}}{n_p},$$

where n_p is a total number of evaluations for the problem p . Thus, $\rho_a(\tau)$ defines the fraction of problems in which the a -th algorithm has an error not more than τ times bigger than the best competitor in the chosen performance metric. Intuitively, the higher is the curve, the better the performance of the corresponding method is, while $\rho_a(1)$ gives the fraction of points for which algorithm a gives the best results among all the considered methods.

The results are shown in Figure 5, where we compare the performance of considered approaches for single NNs with uncertainty estimation by an ensemble of 5 neural networks trained from different random initializations. We observe that all the proposed methods improve over MC dropout, while k-DPP even outperforms the ensemble. Thus, by tuning inference for a single network, we achieve the results which are better than the ensemble approach,

which requires much more resources for training and storing the models.

Additionally we explore an option of further improvement of results by considering ensembles of NNs with tuned inference procedures. Figure 6 shows that ensembles of NNs with diversified sampling allows to improve over the standard ensembles already with significant margin while ensembling models with MC dropout does not help at all.

Considering the log-likelihood metric we show the more refined results for each dataset, see Figure 7. We observe that there is no single method which gives the best results uniformly over the considered datasets, but still, DPP shows superior performance more often than other methods.

Additional results concerning ensembles of models and different variations of NNs, see Supplementary Material.

3.4 Classification

3.4.1 Uncertainty Estimation for Classification

In this section, we aim to show the applicability of the proposed methods to the classification tasks, computer vision problems in particular. We follow the experiment setting from [Hendrycks and Gimpel, 2016], which proposes to assess the quality of UE models by treating them as wrong prediction detectors. Specifically, we expect that the estimated uncertainty on the wrongly labeled samples will be higher compared to UEs for the correctly classified samples. Thus, we can interpret the uncertainty as prediction for the correct/incorrect binary classification problem, and we report ROC-AUC metric on the validation set. We consider three datasets: MNIST, which is a toy dataset of handwritten digits [LeCun, 1998], SVHN, which is also a number classification dataset, but for real-world images [Netzer et al., 2011], and CIFAR-10, which is a 10-class image dataset for simple objects [Krizhevsky et al., 2009].

For the MNIST dataset, we use a simple convolutional neural network with two convolutional layers, max-pooling and two fully connected layers. A dropout rate $p = 0.5$ is used between fully connected layers. For the SVHN and CIFAR-10 we use *resnet-18* for 10 classes and a dropout rate $p = 0.5$ before the last fully-connected layer. We take *variation ratio* as an uncertainty estimate for classification, which was shown to provide good performance as an acquisition function in active learning setting [Beluch et al., 2018].

The experiments are repeated five times with different data splits for each dataset. The results are summarized in Figure 8. It can clearly be seen that the proposed diversification methods outperform MC dropout, while

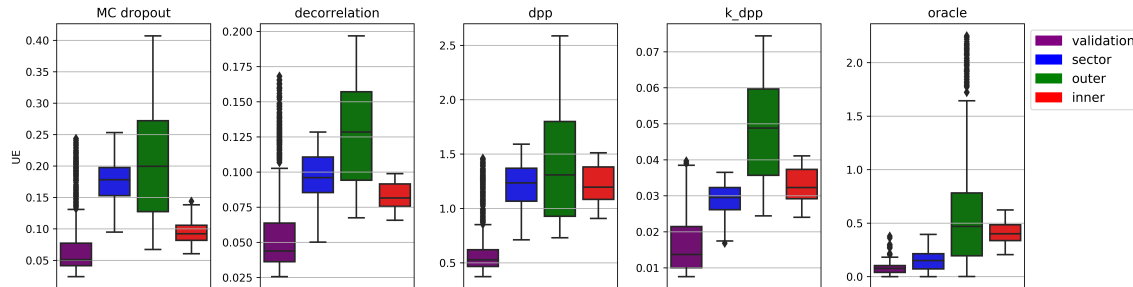


Figure 4: 2D Rings Toy Problem. NAE@10% for various uncertainty estimators for different kinds of OOD data. All of the proposed approaches show better distinction of the inner region points compared to the MC dropout baseline. k-DPP results are more consistent with oracle errors of the neural network compared to other methods.

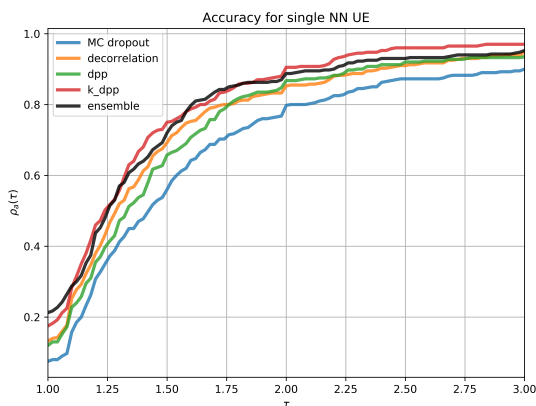


Figure 5: Dolan-More performance curves for the accuracy (hitting top 10% by UE ranking) metric across various UCI datasets for single NN UE models. Rank-DPP demonstrates the performance comparable to the ensemble of 5 NNs.

DPP gives consistently better results with a significant margin.

3.4.2 Active Learning

To further validate the utility of various uncertainty estimates, we consider the problem of active learning. In this scenario, we have a relatively small training set and a large unlabeled pool set, which we are allowed to sample from. Then we make a few iterations, at each iteration we label new samples from the pool set and add them to the training set. Labeling samples from the pool is supposed to be expensive, for example, a manual labeling of the images. Uncertainty estimation methods can help to choose more effectively and speed up the training process.

We conduct our experiments in the setting described

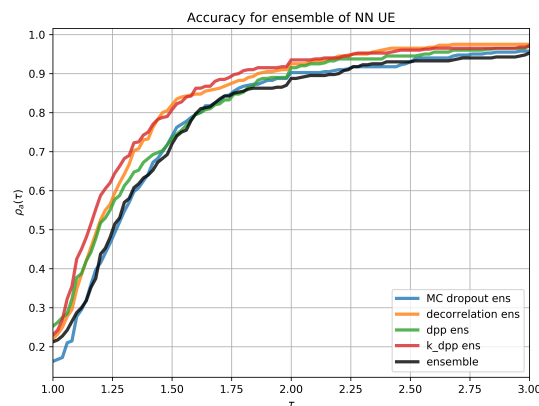


Figure 6: Dolan-More performance curves for the accuracy (hitting top 10% by UE ranking) metric across various UCI datasets for the ensemble of NN UE models. Rank-DPP demonstrates the performance comparable to the ensemble. Moreover, the ensemble of masked NNs could further improve the UE.

in [Gal et al., 2017]. We take MNIST dataset with a small starting training set of 100 samples and take 20 extra samples on each step. We consider the following sampling approaches:

- *Random sampling* – take new samples from the pool uniformly at random;
- *Maximum entropy* – evaluate entropy on softmax prediction by model and take the samples with the highest entropy;
- *Variance ratio* – compute the variance ratio and take the samples with the largest value of this statistic. We compute variance ratios for different considered uncertainty estimation methods.

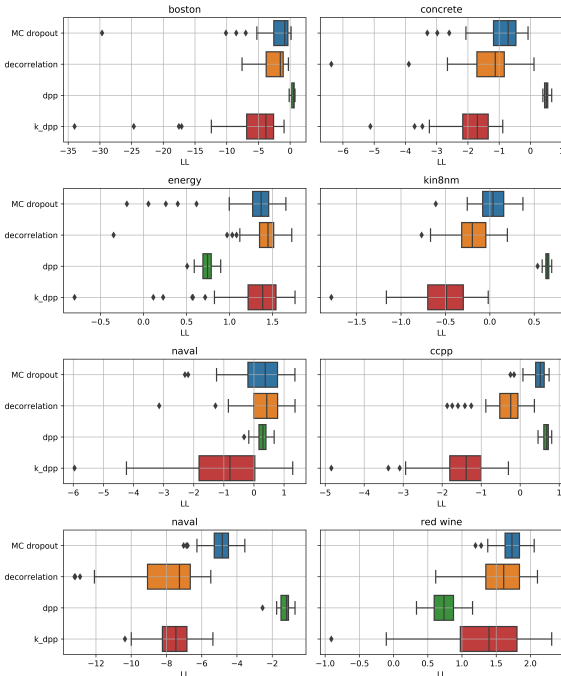


Figure 7: Log-likelihood metric across various UCI datasets for NN UE models. DPP gives reasonable results compared to other methods for most of the datasets.

We also consider “oracle error” sampling – with this method we took the points with the highest error. It cannot be applied in real-life scenario as we do not have access to labels for the pool, but we put it as a reference.

The results are presented in Figure 9. We observe that approaches based on the variance ratio give much better results compared to the max entropy and random sampling baselines. However, we do not see an improvement from the proposed diversification approaches over MC dropout. One possible explanation is that even oracle sampling is not that much better, so the room for improvement here is very limited.

4 Related Work

Dropout [Hinton et al., 2012, Srivastava et al., 2014] has emerged in recent years as a technique to prevent the overfitting in deep and overparametrized neural networks. Over the years, it obtained theoretical explanations as an averaged ensembling technique [Srivastava et al., 2014], a Bernoulli realization of the corresponding Bayesian neural network [Gal and Ghahramani, 2016] and a latent variable model [Maeda, 2014]. It was shown in [Gal, 2016, Nalisnick et al., 2019] that using dropout at the prediction stage (i.e., stochastic forward passes of the test samples through the network, also referred to as *MC dropout*)

leads to unbiased Monte-Carlo estimates of the mean and variance for the corresponding Bayesian neural network trained using variational inference. These uncertainty estimates were shown to be efficient in different scenarios [Gal, 2016, Tsymbalov et al., 2018].

Training an ensemble of models and uncertainty estimation by their disagreement is another common approach [Lakshminarayanan et al., 2017]. It is shown that with few models in an ensemble, you can get robust and useful calibrated results [Beluch et al., 2018], outperforming MC dropout in active learning and error detection. The main disadvantage of ensembles is the necessity to train multiple model instances. However, it was addressed in recent works [Maddox et al., 2019, Garipov et al., 2018, Izmailov et al., 2019] which consider different strategies for speeding up ensemble construction. Recently, it was shown that improving diversity of ensemble members improves the quality of the resulting uncertainty estimates [Jain et al., 2019].

5 Conclusions

We have proposed a new approach that strengthens the dropout-based uncertainty estimation for neural networks. Instead of randomly sampling the dropout masks on the inference stage, we sample special sets of diverse masks via determinantal point processes that utilize the information about the correlations of neurons in the inner layers. Numerical experiments on a wide range of tasks – regression, classification, and active learning – show that our approach outperforms the MC dropout baseline and is competitive with ensemble-based uncertainty estimates. A combination of dropout-based inference with ensembling of several models allows to further improve the quality of the proposed uncertainty estimates and achieve state-of-the-art performance. From the practical perspective, our method is simple to implement as it does not require any modifications to the neural network architecture and the training process.

We expect that the proposed methods of dropout mask sampling may also be used on the training stage, leading to more robust and efficient models. Another compelling direction of further research is approximate DPP sampling, which may increase the sampling speed of the proposed approaches, making them more production-friendly.

The code reproducing the experiments is available at <https://github.com/stat-ml/dpp-dropout-uncertainty>.

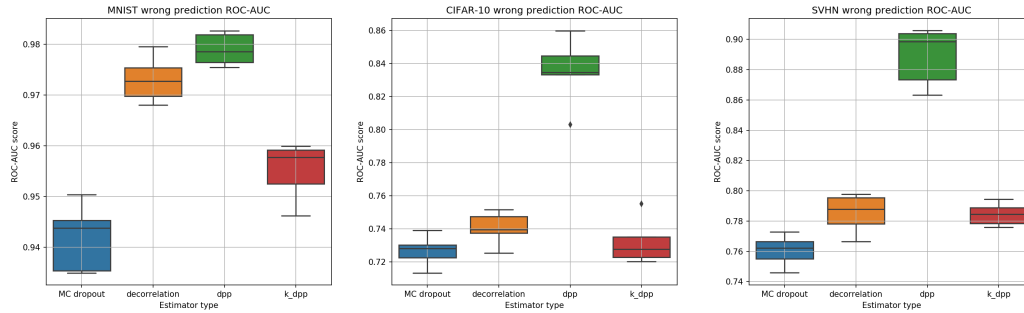


Figure 8: Wrong prediction detection for image classification datasets. We consider the uncertainty estimate as a prediction for the wrong labels on the validation dataset and report ROC-AUC score on this synthetic binary classification.

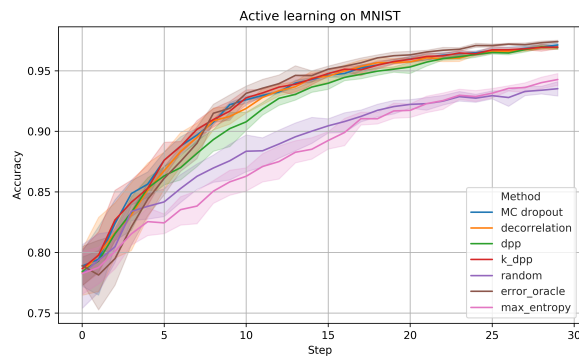


Figure 9: Active learning on MNIST. We start with the small training set and extend it on each step by samples with the highest uncertainty. It allows training with the small amount of labeled data.

Acknowledgements

The authors want to thank Nikita Mokrov for useful discussions. E.T. was supported by the Skoltech NGP Program No. 2016-7/NGP (a Skoltech-MIT joint project) and also acknowledges the usage of the Magnus computational platform by the Skoltech CEST Multiscale Molecular Modelling group (Prof. Alexander Shapeev) for obtaining the part of results presented in this paper. M.P. and K.F. acknowledge the use of “Zhores” super-computer [Zacharov et al., 2019] for obtaining the part of results presented in this paper.

References

[Begoli et al., 2019] Begoli, E., Bhattacharya, T., and Kusnezov, D. (2019). The need for uncertainty quantification in machine-assisted medical decision making. *Nature Machine Intelligence*, 1(1):20–23.

[Beluch et al., 2018] Beluch, W. H., Genewein, T., Nürnberger, A., and Köhler, J. M. (2018). The power of ensembles for active learning in image classification. In *Proceedings CVPR*, pages 9368–9377.

[Çivril and Magdon-Ismail, 2009] Çivril, A. and Magdon-Ismail, M. (2009). On selecting a maximum volume sub-matrix of a matrix and related problems. *Theoretical Computer Science*, 410(47-49):4801–4811.

[Dolan and Moré, 2002] Dolan, E. D. and Moré, J. J. (2002). Benchmarking optimization software with performance profiles. *Mathematical programming*, 91(2):201–213.

[Dua and Taniskidou, 2017] Dua, D. and Taniskidou, E. K. (2017). Uci machine learning repository [<http://archive.ics.uci.edu/ml>].

[Feng et al., 2018] Feng, D., Rosenbaum, L., and Dietmayer, K. (2018). Towards safe autonomous driving: Capture uncertainty in the deep neural network for lidar 3d vehicle detection. In *21st International Conference on Intelligent Transportation Systems (ITSC)*, pages 3266–3273.

[Freeman, 1965] Freeman, L. C. (1965). *Elementary applied statistics: for students in behavioral science*. John Wiley & Sons.

[Gal, 2016] Gal, Y. (2016). Uncertainty in deep learning. *University of Cambridge*.

[Gal and Ghahramani, 2016] Gal, Y. and Ghahramani, Z. (2016). Dropout as a bayesian approximation: Representing model uncertainty in deep learning. In *Proc. ICML’16*, pages 1050–1059.

[Gal et al., 2017] Gal, Y., Islam, R., and Ghahramani, Z. (2017). Deep bayesian active learning with image data.

- In *Proceedings of the 34th International Conference on Machine Learning-Volume 70*, pages 1183–1192.
- [Garipov et al., 2018] Garipov, T., Izmailov, P., Podoprikin, D., Vetrov, D. P., and Wilson, A. G. (2018). Loss surfaces, mode connectivity, and fast ensembling of dnns. In *Advances in Neural Information Processing Systems*, pages 8789–8798.
- [Gautier et al., 2019] Gautier, G., Polito, G., Bardenet, R., and Valko, M. (2019). Dppy: Dpp sampling with python. *JMLR*, 20(180):1–7.
- [Goreinov et al., 2010] Goreinov, S. A., Oseledets, I. V., Savostyanov, D. V., Tyrtshnikov, E. E., and Zamarashkin, N. L. (2010). How to find a good submatrix. In *Matrix Methods: Theory, Algorithms And Applications: Dedicated to the Memory of Gene Golub*, pages 247–256. World Scientific.
- [Guo et al., 2017] Guo, C., Pleiss, G., Sun, Y., and Weinberger, K. Q. (2017). On calibration of modern neural networks. In *Proceedings ICML*, page 13211330.
- [Hendrycks and Gimpel, 2016] Hendrycks, D. and Gimpel, K. (2016). A baseline for detecting misclassified and out-of-distribution examples in neural networks. *arXiv preprint arXiv:1610.02136*.
- [Hernández-Lobato and Adams, 2015] Hernández-Lobato, J. M. and Adams, R. (2015). Probabilistic backpropagation for scalable learning of bayesian neural networks. In *International Conference on Machine Learning*, pages 1861–1869.
- [Hinton et al., 2012] Hinton, G. E., Srivastava, N., Krizhevsky, A., Sutskever, I., and Salakhutdinov, R. R. (2012). Improving neural networks by preventing co-adaptation of feature detectors. *arXiv:1207.0580*.
- [Houlsby et al., 2011] Houlsby, N., Huszár, F., Ghahramani, Z., and Lengyel, M. (2011). Bayesian active learning for classification and preference learning. *arXiv preprint arXiv:1112.5745*.
- [Izmailov et al., 2019] Izmailov, P., Maddox, W., Kirichenko, P., Garipov, T., Vetrov, D., and Wilson, A. G. (2019). Subspace inference for bayesian deep learning.
- [Jain et al., 2019] Jain, S., Liu, G., Mueller, J., and Gifford, D. (2019). Maximizing overall diversity for improved uncertainty estimates in deep ensembles. *arXiv preprint arXiv:1906.07380*.
- [Krizhevsky et al., 2009] Krizhevsky, A., Hinton, G., et al. (2009). Learning multiple layers of features from tiny images.
- [Kulesza et al., 2012] Kulesza, A., Taskar, B., et al. (2012). Determinantal point processes for machine learning. *Foundations and Trends® in Machine Learning*, 5(2–3):123–286.
- [Lakshminarayanan et al., 2017] Lakshminarayanan, B., Pritzel, A., and Blundell, C. (2017). Simple and scalable predictive uncertainty estimation using deep ensembles. In *Advances in neural information processing systems*, pages 6402–6413.
- [LeCun, 1998] LeCun, Y. (1998). The mnist database of handwritten digits. <http://yann.lecun.com/exdb/mnist/>.
- [Maas et al., 2013] Maas, A. L., Hannun, A. Y., and Ng, A. Y. (2013). Rectifier nonlinearities improve neural network acoustic models. In *Proc. ICML'13*, volume 30, page 3.
- [Macchi, 1975] Macchi, O. (1975). The coincidence approach to stochastic point processes. *Advances in Applied Probability*, 7(1):83–122.
- [Maddox et al., 2019] Maddox, W. J., Izmailov, P., Garipov, T., Vetrov, D. P., and Wilson, A. G. (2019). A simple baseline for bayesian uncertainty in deep learning. In *NeurIPS*, pages 13132–13143.
- [Maeda, 2014] Maeda, S.-i. (2014). A bayesian encourages dropout. *arXiv:1412.7003*.
- [Nalisnick et al., 2019] Nalisnick, E., Hernandez-Lobato, J. M., and Smyth, P. (2019). Dropout as a structured shrinkage prior. In *International Conference on Machine Learning*, pages 4712–4722.
- [Netzer et al., 2011] Netzer, Y., Wang, T., Coates, A., Bissacco, A., Wu, B., and Ng, A. Y. (2011). Reading digits in natural images with unsupervised feature learning.
- [Settles, 2012] Settles, B. (2012). Active learning. *Synthesis Lectures on Artificial Intelligence and Machine Learning*, 6(1):1–114.
- [Shannon, 1948] Shannon, C. E. (1948). A mathematical theory of communication. *Bell Syst. Tech. J.*, 27:379–423.
- [Smith et al., 2018] Smith, J. S., Nebgen, B., Lubbers, N., Isayev, O., and Roitberg, A. E. (2018). Less is more: Sampling chemical space with active learning. *The Journal of chemical physics*, 148(24):241733.
- [Snoek et al., 2019] Snoek, J., Ovadia, Y., Fertig, E., Lakshminarayanan, B., Nowozin, S., Sculley, D., Dillon, J., Ren, J., and Nado, Z. (2019). Can you trust

your model’s uncertainty? evaluating predictive uncertainty under dataset shift. In *Advances in Neural Information Processing Systems*, pages 13969–13980.

[Srivastava et al., 2014] Srivastava, N., Hinton, G., Krizhevsky, A., Sutskever, I., and Salakhutdinov, R. (2014). Dropout: A simple way to prevent neural networks from overfitting. *The Journal of Machine Learning Research*, 15(1):1929–1958.

[Tsymbalov et al., 2018] Tsymbalov, E., Panov, M., and Shapeev, A. (2018). Dropout-based active learning for regression. In *International Conference on Analysis of Images, Social Networks and Texts*, pages 247–258.

[Vyas et al., 2018] Vyas, A., Jammalamadaka, N., Zhu, X., Das, D., Kaul, B., and Willke, T. L. (2018). Out-of-distribution detection using an ensemble of self-supervised leave-out classifiers. In *Proceedings ECCV*, pages 550–564.

[Zacharov et al., 2019] Zacharov, I., Arslanov, R., Gunin, M., Stefonishin, D., Bykov, A., Pavlov, S., Panarin, O., Maliutin, A., Rykovanov, S., and Fedorov, M. (2019). zhorespetaflops supercomputer for data-driven modeling, machine learning and artificial intelligence installed in skolkovo institute of science and technology. *Open Engineering*, 9(1):512–520.

Supplementary Material

A: Different NN Configurations on UCI Regression Datasets

In order to testify UE approaches on a slightly different settings of NN architecture, we settled out three more experiments with variations in:

- **architecture.** Different problems require different fully-connected layers of NNs to be used in order to being able both train on data successfully and do not overfit.
- **activation function.** It was shown² that the choice of activation function may alter the confidence of the predictions on the OOD data. To that end, we considered both linear and non-linear rectifiers.
- **dropout rate.** While in classic papers the most robust dropout rate $p = 0.5$ is often considered, for real problems lesser values of p are used in order to speed up the convergence and smaller NNs to be used. Initially³, the dropout rate is proposed to be chosen in a cross-validation round together with other hyperparameters, such as regularization term, learning rate, etc.

The variations in the settings are provided in Table 2, with the results of Experiment A provided in the main text.

Table 2: Settings for UCI experiments.

Index	Architecture	Activation	p
A (main text)	128-128-64	leaky ReLU	0.5
B	32-32-16	leaky ReLU	0.5
C	128-128-256	CELU	0.2
D	256-256-512	CELU	0.5

To represent our results in a compact form of tables, we are focusing on the following metrics here:

- log likelihood (LL);
- $\rho_a(1)$, also called as *efficiency* of algorithm a , is the number of problems for which algorithm a is one of the best. We do not provide the *robustness* $\rho_a(\tau_{max})$, as it is not differ much among the algorithms in our settings.

²Hein, Matthias, Maksym Andriushchenko, and Julian Bitterwolf. "Why ReLU networks yield high-confidence predictions far away from the training data and how to mitigate the problem." Proceedings of the IEEE Conference on Computer Vision and Pattern Recognition. 2019.

³Gal, Yarin. "Uncertainty in deep learning." University of Cambridge

- $I(\tau_{max}) = \int_1^{\tau_{max}} \rho_a(\tau) d\tau$ is an integral metric, which represents the volume under the performance curve.

The results for the last two metrics are shown in Table 3. It is clear that DPP-powered ensembles shows the best performance compared to the other ensembles. In the case of single NN UE, k-DPP also shows superior performance in Experiments A and B, yet for larger NNs (Experiments C and D), the MC dropout hits the top; we suppose that this may be connected to the overfitting of a relatively large NNs on a small datasets we use in our experiments. Please note that Table 2 does not allow a direct comparison between single models and ensembles as well as comparison with the Figures 5 and 6 due to competitive nature of the performance curves.

Table 3: Performance-based metrics for the Experiments A-D. DPP-powered ensembles shows the best performance compared to the other ensembles; in case of single NN UE k-DPP is preferable for the relatively small NNs.

Experiment	A		B		C		D	
Single NN	$\rho_a(1)$	$I(3)$	$\rho_a(1)$	$I(3)$	$\rho_a(1)$	$I(3)$	$\rho_a(1)$	$I(3)$
MC dropout	0.228	1.603	0.336	1.750	0.427	1.817	0.423	1.795
decorrelation	0.343	1.769	0.420	1.786	0.280	1.628	0.420	1.733
DPP	0.352	1.738	0.368	1.713	0.320	1.744	0.309	1.739
k-DPP	0.487	1.850	0.536	1.875	0.380	1.785	0.286	1.757
Ensembles								
MC dropout	0.225	1.648	0.352	1.773	0.270	1.752	0.311	1.709
decorrelation	0.295	1.742	0.460	1.873	0.305	1.729	0.354	1.784
DPP	0.333	1.700	0.308	1.751	0.417	1.796	0.449	1.784
k-DPP	0.325	1.759	0.544	1.914	0.265	1.764	0.234	1.690
ensemble	0.292	1.641	0.128	1.425	0.195	1.604	0.206	1.507

The results for LL metric are shown in Tables 4, 5, 6 and 7. For most of the datasets, DPP-based algorithms show promising results with a few exceptions.

B: LL for Ensembles on UCI Datasets.

In the light of Experiment A, we visualize the log-likelihood metric for each dataset, see Figure 10. There is no single method which gives the best results uniformly over the considered datasets, yet DPP or MC dropout ensembles show superior performance more often than other methods.

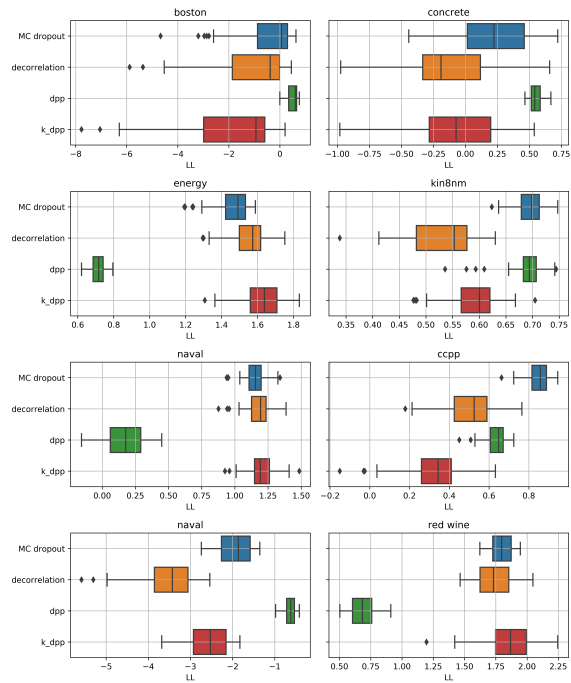


Figure 10: Log-likelihood across various UCI datasets for ensembles of NN UE models.

Table 4: Log likelihoods for the experiment A (main text). Bold font indicates the best method based on a mean LL value.

Algorithm	boston	ccpp	concrete	energy	kin8nm	naval	red wine	yacht
MC dropout	-2.31 ± 4.545	0.472 ± 0.204	-0.895 ± 0.692	1.254 ± 0.378	0.036 ± 0.17	0.198 ± 0.806	-4.916 ± 0.791	1.715 ± 0.187
decorrelation	-2.496 ± 2.025	-0.369 ± 0.501	-1.382 ± 1.003	1.383 ± 0.294	-0.213 ± 0.226	0.27 ± 0.762	-7.977 ± 2.025	1.573 ± 0.35
DPP	0.451 ± 0.249	0.659 ± 0.091	0.51 ± 0.066	0.738 ± 0.078	0.646 ± 0.03	0.264 ± 0.204	1.26 ± 0.323	0.737 ± 0.178
k-DPP	-6.157 ± 6.223	-1.536 ± 0.841	-1.884 ± 0.821	1.266 ± 0.466	-0.525 ± 0.327	-1.021 ± 1.428	-7.534 ± 1.104	1.287 ± 0.732
MC dropout ens.	-0.522 ± 1.247	0.849 ± 0.062	0.209 ± 0.301	1.462 ± 0.1	0.696 ± 0.027	1.154 ± 0.087	-1.918 ± 0.373	1.794 ± 0.088
decorrelation ens.	-1.173 ± 1.622	0.502 ± 0.126	-0.149 ± 0.35	1.553 ± 0.108	0.534 ± 0.063	1.18 ± 0.102	-3.555 ± 0.702	1.747 ± 0.148
DPP ens.	0.517 ± 0.2	0.636 ± 0.061	0.553 ± 0.051	0.712 ± 0.044	0.688 ± 0.039	0.164 ± 0.162	-0.64 ± 0.138	0.681 ± 0.099
k-DPP ens.	-1.961 ± 2.01	0.314 ± 0.161	-0.072 ± 0.364	1.624 ± 0.123	0.589 ± 0.052	1.202 ± 0.108	-2.586 ± 0.473	1.859 ± 0.202
ensemble	-15.207 ± 27.01	-7.551 ± 3.256	-7.031 ± 4.416	-0.691 ± 2.05	-3.159 ± 0.652	0.812 ± 0.475	-15.351 ± 4.33	1.031 ± 2.034

Table 5: Log likelihoods for the experiment B. Bold font indicates the best method based on a mean LL value.

Algorithm	boston	concrete	energy	red wine	yacht
MC dropout	-0.706 ± 1.404	-1.041 ± 0.66	0.941 ± 0.351	-2.847 ± 0.494	1.277 ± 0.171
decorrelation	-1.595 ± 2.262	-0.985 ± 0.904	1.039 ± 0.258	-4.239 ± 1.794	1.31 ± 0.214
DPP	0.464 ± 0.14	0.383 ± 0.068	0.42 ± 0.085	-0.862 ± 0.208	0.376 ± 0.18
k-DPP	-5.355 ± 6.531	-3.721 ± 1.772	0.366 ± 0.897	-5.117 ± 0.835	1.075 ± 0.73
MC dropout ens.	0.462 ± 0.317	0.38 ± 0.095	1.125 ± 0.035	-1.05 ± 0.143	1.353 ± 0.062
decorrelation ens.	0.208 ± 0.567	0.313 ± 0.145	1.225 ± 0.057	-1.73 ± 0.253	1.383 ± 0.108
DPP ens.	0.516 ± 0.095	0.403 ± 0.054	0.399 ± 0.047	-0.409 ± 0.064	0.317 ± 0.158
k-DPP ens.	-0.123 ± 0.601	0.042 ± 0.164	1.336 ± 0.094	-1.682 ± 0.243	1.617 ± 0.156
ensemble	-6.891 ± 2.919	-7.039 ± 4.122	-1.664 ± 1.592	-11.754 ± 2.938	-1.489 ± 3.501

Table 6: Log likelihoods for the experiment C. Bold font indicates the best method based on a mean LL value.

Algorithm	boston	ccpp	concrete	energy	kin8nm	naval	red wine	yacht
MC dropout	-2.337 ± 1.353	-5.623 ± 1.55	-2.606 ± 1.314	1.153 ± 0.283	-0.22 ± 0.545	-0.853 ± 1.75	-5.313 ± 0.575	1.667 ± 0.464
decorrelation	-2.691 ± 1.648	-5.958 ± 1.858	-4.658 ± 1.886	1.096 ± 0.305	-1.474 ± 0.844	-1.302 ± 2.151	-6.216 ± 0.79	1.608 ± 0.509
DPP	0.326 ± 0.095	0.63 ± 0.086	0.308 ± 0.074	0.367 ± 0.135	0.612 ± 0.048	-0.32 ± 0.134	-0.422 ± 0.046	0.896 ± 0.098
k-DPP	-4.392 ± 1.954	-237.32 ± 93.705	-4.253 ± 1.865	-0.486 ± 1.13	-0.759 ± 0.777	-1.992 ± 2.477	-6.539 ± 0.725	-11.601 ± 13.149
MC dropout ens.	-0.171 ± 0.494	-1.148 ± 0.531	0.245 ± 0.193	1.497 ± 0.095	0.67 ± 0.096	1.182 ± 0.098	-2.195 ± 0.283	1.92 ± 0.128
decorrelation ens.	-1.081 ± 0.804	-2.626 ± 0.887	-1.741 ± 0.607	1.481 ± 0.116	-0.444 ± 0.283	1.311 ± 0.198	-4.044 ± 0.38	1.898 ± 0.225
DPP ens.	0.324 ± 0.071	0.642 ± 0.045	0.327 ± 0.056	0.337 ± 0.061	0.641 ± 0.03	-0.373 ± 0.073	-0.403 ± 0.031	0.885 ± 0.063
k-DPP ens.	-1.33 ± 0.808	-5.387 ± 2.189	-0.194 ± 0.329	1.378 ± 0.217	0.563 ± 0.125	1.245 ± 0.11	-2.51 ± 0.299	1.93 ± 0.407
ensemble	-6.071 ± 4.715	-7.616 ± 5.913	-1.428 ± 0.989	0.601 ± 2.216	-2.421 ± 1.321	1.123 ± 0.373	-10.693 ± 3.31	1.362 ± 3.911

Table 7: Log likelihoods for the experiment D. Bold font indicates the best method based on a mean LL value.

Algorithm	boston	concrete	energy	kin8nm	naval	red wine	yacht
MC dropout	-0.918 ± 0.815	-1.413 ± 0.885	0.577 ± 0.691	-0.339 ± 0.955	-0.48 ± 1.419	-5.799 ± 1.73	1.463 ± 0.269
decorrelation	-2.619 ± 1.348	-4.664 ± 1.783	-0.056 ± 1.183	-2.45 ± 2.025	-2.891 ± 3.017	-10.623 ± 2.725	1.364 ± 0.53
DPP	0.374 ± 0.083	-0.031 ± 0.084	0.517 ± 0.111	0.549 ± 0.161	0.122 ± 0.129	-0.464 ± 0.095	0.683 ± 0.092
k-DPP	-12.525 ± 5.184	-9.068 ± 3.009	-13.063 ± 16.753	-2.24 ± 2.041	-6.901 ± 6.479	-8.833 ± 2.141	-17.552 ± 13.365
MC dropout ens.	0.325 ± 0.258	0.336 ± 0.111	1.246 ± 0.057	0.73 ± 0.148	0.968 ± 0.099	-2.023 ± 0.45	1.571 ± 0.074
decorrelation ens.	-0.828 ± 0.473	-1.044 ± 0.451	1.277 ± 0.158	-0.225 ± 0.491	1.04 ± 0.386	-5.184 ± 1.04	1.858 ± 0.186
DPP ens.	0.421 ± 0.061	0.011 ± 0.041	0.545 ± 0.059	0.74 ± 0.044	0.165 ± 0.062	-0.348 ± 0.054	0.69 ± 0.057
k-DPP ens.	-3.829 ± 1.433	-1.893 ± 0.672	0.487 ± 0.518	0.387 ± 0.392	0.987 ± 0.44	-2.912 ± 0.646	1.882 ± 0.385
ensemble	-3.655 ± 5.261	-0.734 ± 0.737	0.965 ± 0.877	-0.739 ± 1.285	1.005 ± 0.206	-8.445 ± 4.316	1.434 ± 1.738